Tip-enhanced Raman scattering

Elena Bailo[a] and Volker Deckert*[ab]

Received 17th March 2008
First published as an Advance Article on the web 31st March 2008
DOI: 10.1039/b705967c

Tip-enhanced Raman scattering (TERS) is a technique that provides molecular information on the nanometre scale. Using a nanometre-sized metal particle results in a strong signal enhancement and a lateral resolution similar to the dimensions of the particle. As TERS is in a way the ultimate SERS experiment, the theoretical background will be briefly discussed with respect to the unique features and the specific effects that occur when only a single nanoparticle is used as a probe. All the major parts of the instrument will be revealed and the specific advantages of the different instrumental set ups will be investigated with respect to the particular requirements of the sample. Selected examples ranging from material science to cell biological applications demonstrate the capabilities and the potential of TERS in this *tutorial review*.

After the discovery of surface-enhanced Raman scattering (SERS), a new era started for Raman spectroscopy. SERS research inspired Raman spectroscopy and is still motivating the development of the technique 30 years later.

While the general sensitivity of SERS is not the question, the main obstacle when using SERS for the investigation of interfaces is the inhomogeneity of the SERS substrate across the sample. The different shapes, sizes and roughness of single particles and clusters result in strong variations in the field enhancement and consequently the Raman signal. Furthermore, these physical parameters also depend critically on the substrate preparation. Therefore, a spatially resolved quantitative analysis of interfaces using SERS is impossible.

It is well known that the large field enhancement at metal particles occurs in regions of high curvature and maximum enhancement occurs for elongated particles with dimensions of about 10–100 nm. While clusters are considered to yield a better overall enhancement, a single isolated metal nanoparticle can also enhance the field considerably.[1–5]

Wessel[3] proposed a scheme to ensure a constant field enhancement using just one single metal nanoparticle for the investigation of a surface. This introduced for the first time the potential of quantitative SERS surface analysis. In this design the rough metal film was replaced by a sharp metal tip that should act as an exclusive active site, which also represents the limit for any SERS experiment—at least one particle is required. The tip should then be scanned over the sample surface using scanning probe microscopy (SPM) techniques. The later experimental verification of this now called *T*ip-*E*nhanced *R*aman *S*cattering (TERS) proved that, in addition to the field enhancement, the lateral resolution of the method was also improved down to 10 nm, due to the small size of the probe.[6–10]

At present, this combination of SPM techniques and Raman spectroscopy is successfully applied to many questions in the nano-sciences because of its unique possibility to provide chemical and structural information on a sample surface with highest lateral resolution combined with high sensitivity.

[a] *ISAS – Institute for Analytical Sciences, Bunsen-Kirchhoff-Str. 11, 44139 Dortmund, Germany. E-mail: deckert@isas.de; Fax: +49 231 1392 120; Tel: +49 231 1392 218*
[b] *Technische Universität Dortmund, Physical Chemistry, Otto-Hahn-Str. 6, 44227 Dortmund, Germany*

Elena Bailo studied chemistry at the University of Barcelona and received her diploma in analytical chemistry in 2005. Since 2006, she has been doing her PhD thesis, working on "DNA sequencing by tip-enhanced Raman scattering (TERS)" under the supervision of PD Dr. Volker Deckert at ISAS – Institute for Analytical Sciences, Dortmund, Germany.

Volker Deckert is the Director of the Proteomics Department at the ISAS – Institute for Analytical Sciences in Dortmund, Germany. He obtained his Diploma and PhD from the University of Würzburg (Germany), working in the field of Raman spectroscopy. He was a postdoc at the University of Tokyo and KAST, in Kawasaki, where he worked on non-linear and time-resolved laser spectroscopy. During his habilitation at the ETH Zurich, he worked on near-field optical spectroscopy, a subject he pursues at his current position.

Theoretical background

Electromagnetic field enhancement at single metal particles

The large enhancement in Raman scattering of a single metal probe used in TERS can be discussed on the same basis as the SERS effect. In general, two mechanisms are responsible for the SERS enhancement: the electromagnetic effect and the chemical or charge transfer effect, which applies only to the first layer of adsorbates.

On the surface of spherical and elongated metal nanoparticles, surface plasmons are excited by light. The involved electromagnetic fields can be strongly enhanced in the presence of surface plasmons if certain resonance conditions are fulfilled. The product of the enhancement of the incident laser field and the scattered Raman then yields the overall electromagnetic SERS effect.[1,2]

The second enhancement mechanism, called the chemical effect, corresponds to an amplification in the polarizability of the molecule due to a charge transfer between the metal and the adsorbed molecule.[11,12] Considerable band shifts are associated with this effect and can be used to distinguish whether the metal particle is in direct contact with the sample. Experimental evidence for a chemical effect also exists for TERS experiments on nucleobases and C_{60}, done by the groups of Kawata and Deckert, respectively.[6,13,14] Band shifts on adenine were observed, which strongly indicate direct involvement of a silver–nucleobase interaction and consequently a chemical enhancement. In contrast, no band shifts are detected for a different TERS experiment on cytosine and thymine nanocrystals. This has been attributed to a special distribution of silver nanoparticles on the specific AFM tip used in this TERS experiment. In this case, the silver particle was placed slightly behind the actual apex of the probe but still close enough to the substrate to cause an electromagnetic enhancement. Consequently, no evidence for a direct interaction between tip and specimen in this particular experiment was observed and the spectra therefore resemble essentially the bulk spectra of the nucleobases and not the SERS spectra.[15]

One of the most important features of TERS is the ability to highly confine the electromagnetic field at the apex of a sharp metal tip, firstly due to an electrostatic lightning rod effect as a result of the shape of the particle at the tip apex, and secondly due to surface plasmon resonances which correlate the wavelength of the excitation source and the actual tip geometry. This results in the high spatial resolution of the technique.

Near-field optics

The basic explanation of the high-resolution capabilities of TERS is based on near-field optics and, in particular, in evanescent waves that occur close to small objects. An evanescent wave is a standing wave that exponentially decays in space. It can be probed using a nano-antenna, which converts the standing wave into a propagating wave detectable in the far-field.

The enhancement associated with a TERS tip varies with respect to the specific position on the particle. The electric properties of the material, the size and shape of the metal tip, and the illumination geometry play an important role in the enhancement factor and its distribution around the tip.

Different models have been developed to theoretically investigate the field enhancement of single particles.[9]

In order to calculate the electromagnetic fields involved when a metallic nanoparticle or tip is irradiated with light, one has to solve either Maxwell's or Helmholtz's equations. For this purpose, several numerical methods are available that can be classified as:

- An analytical extension that describes the geometry and solves the field equations as well as the boundary conditions exactly. Neither area nor time should be discretized.

- Semi-analytical methods, where only the field equations are solved exactly within certain domains. The adjustment of the boundary conditions takes place through approximated solutions by discretization of boundary points and minimization of the errors. The multiple multipole (MMP) method is one of those techniques.

- Semi-numerical methods. Here, the boundary conditions are exactly determined and field equations within a domain are solved approximately. In this way, the area is discretized. Two examples of this method are the finite difference time domain (FDTD) method and the finite element method (FEM).

- Full numerical methods. Here, both the boundary conditions and the solutions within the domain are numerically approximated. As a result, the area and the domain boundary are discretized.[16]

FEM, MMP and FDTD are most frequently applied to model the field distribution of single metal nanoparticles and will be discussed in more detail.

By the FDTD method,[17,18] Maxwell's equations are discretized directly in time and space. The domain area is discretized in this case by rectangles (see Fig. 1). The boundary conditions between the elements are exactly adjusted and each block in the interior of the domain is interpolated.

The FE method[19,20] operates in the frequency domain and unlike FDTD, Helmholtz's equations are discretized in the space domain. It uses a continuous domain which is divided into simple polygons as so called subdomains (see Fig. 1).

In MMP,[21,22] the unknown E- and H-fields within individual homogeneous domains are developed by a series expansion in spherical wavelength vectors, called multipoles, using known analytical solutions of Maxwell's equations. The amplitudes of these fields are then solved by a generalized point matching method (GPMM). In general, the scattering problem is described as a set of linear differential equations.

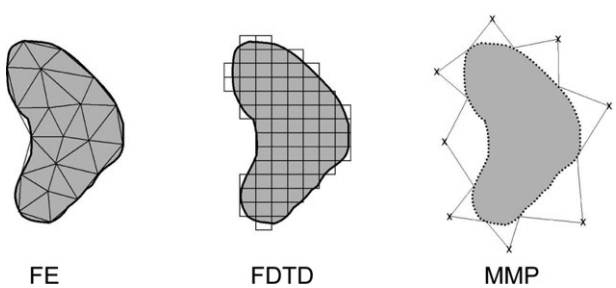

Fig. 1 Different discretization methods used in the theoretical modelling of electromagnetic fields of particles (see text for details).

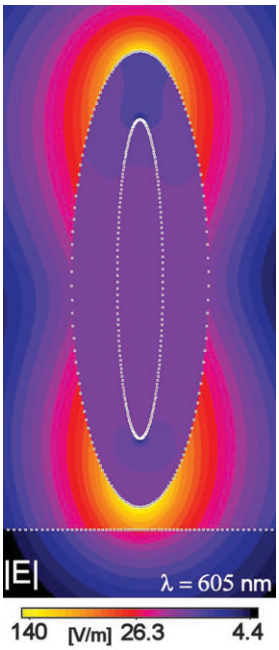

Fig. 2 MMP calculation of the field distribution of an evanescently excited ellipsoidal particle with a glass core.

As an example of the MMP method applied in optical problems, in Fig. 2 the electric field distribution of a silver ellipsoid with a glass core is shown. The particle was excited at its resonance frequency at 605 nm using an evanescent field.[16] The studies can easily be extended to more complex/realistic objects, as shown in Fig. 3. Here the influence of different core shapes on the resonance frequency of a coated silver ellipsoid is shown.[16] Even small changes can cause quite large shifts in the resonance. With respect to the practical experiment this has two aspects. Tips should be carefully checked with respect to the excitation laser wavelength as the plasmon resonances can be far from the desired spectral range. Concerning the tip production, it can provide a nice way of tuning TERS tips towards the desired resonances, if proper conditions are used.

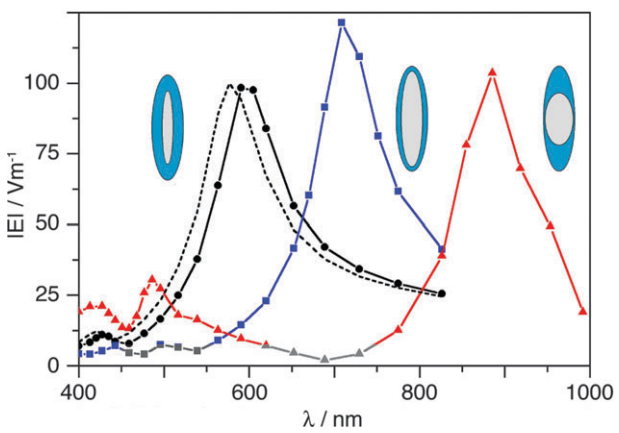

Fig. 3 Wavelength dependency of the field enhancement of ellipsoidal silver particles with different core sizes (calculated using MMP).

Polarization

As previously mentioned, a surface plasmon resonance (SPR) is induced by the electric field of an excitation source (usually a laser). The field enhancement depends critically on the laser beam polarization, which can be also deduced from theoretical modelling as mentioned earlier. If the electric field vector of the incident light is perpendicular (s-polarized) to the metal tip axis, the free electrons are driven to the sides lateral of the tip. As a result the tip apex remains uncharged. But if the electric field vector of the incident light is parallel (p-polarized) to the tip axis, the free electrons on the surface of the metal are confined to the end of the apex of tip (see Fig. 4). As a consequence, the field enhancement is increasing.[22]

In a laser beam, the electric field, E, and the magnetic field, H, oscillate perpendicular to the propagation direction. By focusing with low numerical aperture (NA) lenses, the laser can be approximated as a Gaussian beam and the electric and magnetic fields remain transversal to the axis of the propagation in the focal region. On the other hand, we have to consider that a widely used illumination configuration in TERS at present is the back-reflection mode, which is illuminating the tip from the bottom (other illumination geometries will be discussed in the following sections). This configuration incorporates objective lenses with high numerical aperture (NA) to improve the efficiency of both illumination and collection. In this case, the focus is very confined and the fields are not necessarily perpendicular to the propagation direction.[23] In the tightly focused region orthogonal field vectors appear, in particular E-vector components that are almost parallel to the main propagation direction of the beam. These longitudinal fields appear close to the focal region.[24] When using high NA objective lenses, linearly polarized light is not the best choice because at the center of the focused spot the Z-components of the E-field cancel out. For a back-reflection set-up, a radial polarization mode shows an improvement in the Z-components of the E-field, providing a better tip-enhancement effect, and the background signal decreases because these fields in general match the shape of the tip much better.[25]

For reflection modes using a side illumination configuration, the largest enhancement is achieved when the E-fields of

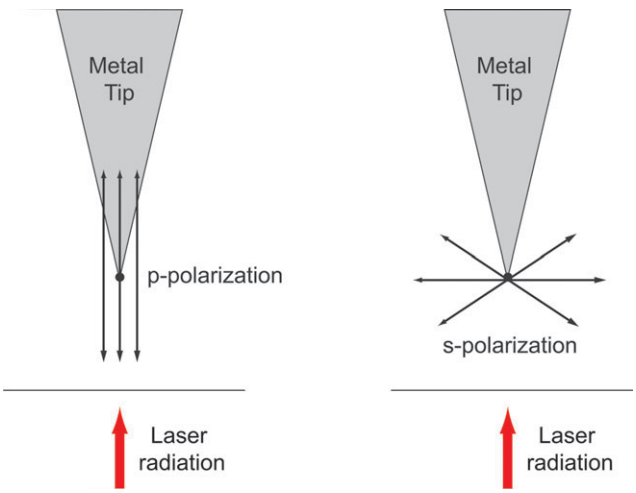

Fig. 4 Schematic diagram of s- and p-polarization at the tip.

the incident radiation are parallel to the tip axis. That is because the near field (close to the vicinity of the tip apex) and far field (from unenhanced Raman, which could be considered as background) contributions show different polarization, so the far-field component will be minimized using a parallel polarization with respect to the tip axis, which furthermore improves the near-field signal.[26,27] For this geometry, the proper illumination conditions are easier to fulfil, the problem is the poorer collection efficiency (NA) of such optical arrangements.

Higher order optical effects

Tip-enhanced near-field optical microscopy is a technique that is mainly applied in combination with linear optical processes like Raman, IR or fluorescence, but the strong field enhancements involved can also induce non-linear optical processes, such as second-harmonic generation (SHG), coherent anti-Stokes Raman scattering (CARS), and hyper-Raman.

Strong parallel E-field components can drive the dipole oscillating at the apex of the tip with a frequency (2ω), twice the frequency of the excitation source (ω). Then, a signal with the same frequency (2ω) at the oscillating dipole is emitted from the tip with an angle (θ) (see Fig. 5). This is known as second-harmonic (SH) radiation.[28,29]

Coherent anti-Stokes Raman scattering (CARS) is a third-order non-linear optical process that, in combination with tip-enhancement optical effect, provides a high spatial resolution and similar information content as Raman spectroscopy.

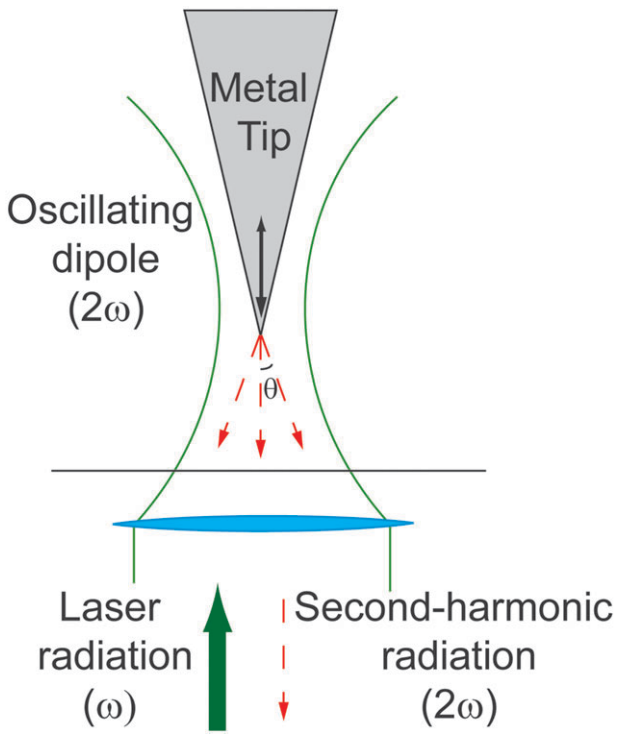

Fig. 5 Schematic diagram of a sharp metal tip which emits second-harmonic (SH) radiation at the critical angle of total internal reflection. SHG radiation is identical to the emission radiation of the dipole oriented vertically on a dielectric substrate.

DNA molecules and single walled carbon nanotubes (SWNTs) have been recently investigated using tip-enhanced-CARS.[30,31]

Another example of a non-linear method that it is applied together with plasmonic metal tips is hyper-Raman scattering (HRS). The observation of IR active bands of SWNTs using hyper-Raman TERS has been clearly demonstrated by Kawata and Uosaki *et al.*[32]

Special effects in TERS

In a conventional Raman experiments, the change in polarizability caused by the electric field of the excitation source is the basis for the spontaneous Raman effect. However, when the applied electric fields vary along a vibrational mode, the generated Raman signal depends directly on the proportional polarizability change. In this case, a polarizability gradient is present and the induced dipole is asymmetric. Therefore, new selection rules have to be considered and vibrations that are usually not Raman active can be observed. Such high field gradients can be induced on the surface of metal nanoparticles. If a sample is close to such a particle, a gradient field Raman (GFR) effect might be achieved. For bonds with a large polarizability, the GFR should become important. That means that vibrational infrared active modes should be detectable under large field gradient conditions, complementing the Raman spectra.[33]

Working with a single nanoparticle and sample features which are even smaller, additional effects can induce changes in band intensities and also in band positions.[34] In normal Raman, such changes can be explained by varying concentrations or different sample compositions. The relationship between the distance dependency for the enhancement between tip and sample is a crucial issue.[21,35,36]

If the field enhancing capabilities of a TERS probe come close to a single molecule detection limit, it is important where the tip comes closest to the molecule. The usual averaging arguments do not hold in this case, because of the limited numbers of scatterers. Furthermore, the normal composition of sample *versus* Ag-tip does not necessarily resemble the computed minimized energy configurations. Tip and sample are "forced" into a certain arrangement. With respect to the measured TERS spectra, it is expected that they will closely resemble normal Raman or SERS spectra. But because of the limited number of molecules, it will be similar to single crystal Raman experiments with an unknown orientation of the sample. Last but not least, the measured spectra do not necessarily reflect the bulk properties of the specimen. This is because the TERS interaction region is confined to only a few nanometres and also the interaction with the substrate must be always considered as well. These small changes can provide additional information for the investigation of surfaces.

Experiment

Instrumentation

The crucial attribute of a TERS experiment is a field enhancing metal feature or particle which is raster scanned across a sample surface.

An essential pre-requisite for any TERS experiment is a scanning probe microscope of some sort to provide a scanning stage that controls precisely the distance between particle and surface. Either AFMs or STMs are presently used for this purpose. While the latter can control the distance more easily, STMs are restricted to either conductive samples or very thin layers of non-conductive samples on a conductive support. This restricts the generality of the method quite severely. For normal AFMs to be general tools, in particular for soft samples, they have to be operated in a non-contact mode of some sort to avoid sample damage. This always induces fluctuations in the optical signal due to the oscillation of the probe necessary to maintain feedback. Therefore a careful balance is required to optimize the TERS setup for a specific experiment.

TERS Experiment

Fig. 6 shows a schematic diagram of a tip-enhanced Raman scattering setup working in back-reflection mode. An inverted Raman microscope is coupled with an AFM for synchronized use. The microscope is required to illuminate the metal coated AFM tip. The back scattered Raman signal is collected through the same objective and notch or edge filter are used to block the laser line. After this filter stage, the signal is coupled to a spectrometer equipped with a cooled charge-coupled device (CCD) for spectrally resolved measurements.

The AFM is placed on the microscope such that the cantilever is roughly aligned with respect to the laser. The final alignment of the cantilever is done by scanning the tip through the laser focus, and collecting the reflected light using a simple photodiode. In Fig. 7, the typical optical response image of a silver coated non-contact AFM tip is shown. This reflectivity image helps to finally position the tip at the position of highest signal intensity and then fix the tip in the x and y directions. At this point the second piezo-stage (sample stage) is activated and only the sample is moved. A piezo actuator synchronizes the microscope objective with the

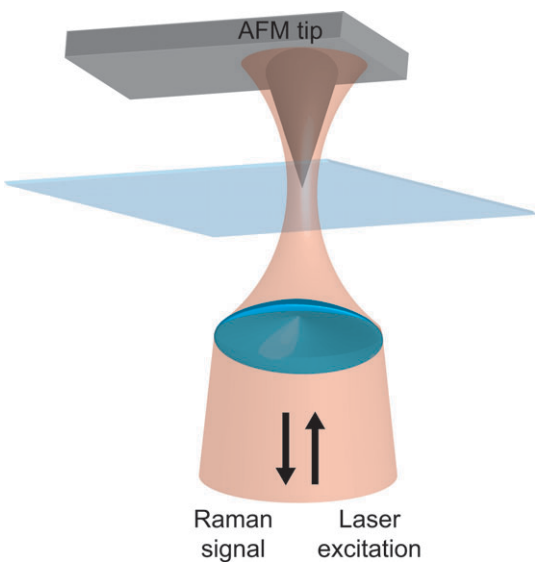

Fig. 6 Schematic diagram of a tip-enhanced Raman scattering setup working in back-reflection mode.

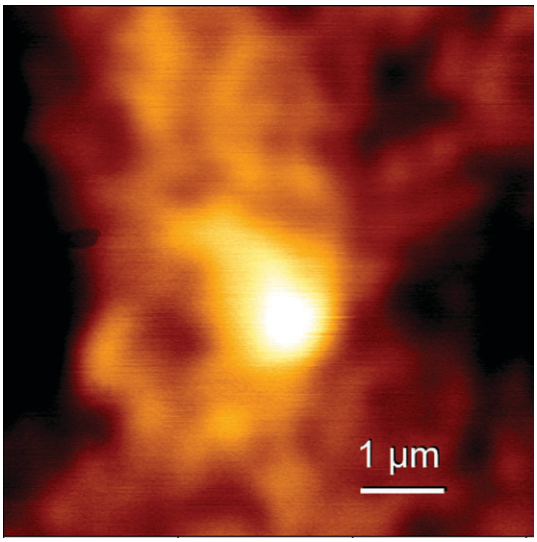

Fig. 7 Optical response of a TERS tip when scanned through the laser focus. The bright spot corresponds to the enhancing area of the tip.

height feedback of the AFM tip to keep the tip always in focus. At this moment point usually several topographic images of the sample are recorded to find sites of interest on the surface for the actual TERS experiment.

Probe preparation

At present, there are several techniques which generate TERS probes with acceptable optical quality, but the reproducibility and yield of good tips are still a challenge. The two techniques most frequently used for TERS probe fabrication are electrochemical etching methods of solid metal probes and the metal evaporation deposition on AFM tips. Both methods will be discussed hereafter.

Pure metal tips. To enhance the Raman signal, mainly metals like gold, silver or copper are used. So far the best TERS enhancement factors have been demonstrated with gold and silver. Compared to normal SERS experiments, gold is used more frequently because gold tips are easy to manufacture. To produce the desired sharp edges required for the TERS experiments, metal wires can be sharpened using electrochemical etching procedures. Many methods have been developed for STM probes, but the overall geometry of the tip is usually less critical in this case. In TERS, a good quality refers to a larger part of the tip because naturally the interaction with the optical fields extends further than the tunnel effect involved in STM.

In the case of gold tips, the electrochemical etching procedures are well established and involve mainly a voltage between a gold wire and a metal ring electrode, both dipped in concentrated hydrochloric acid solution.[37] Between the ring and the gold wire a large surface tension is formed and the etching proceeds more quickly in the meniscus region. During the reaction, the wire becomes thinner until it breaks and falls down. At this moment the electrical circuit is switched off.

Silver in general has better optical properties with respect to the surface enhancement properties than gold. However, a

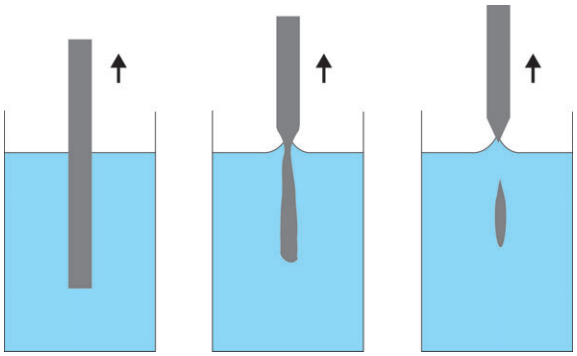

Fig. 8 Schematic diagram of the electrochemical cell for the Ag etching procedure.

different electrochemical etching procedure to prepare sharp silver tips for TERS is required. Mainly two methods are being used. In the first, a silver wire is dipped in a solution of ammonia 10–35%. A stainless steel plate acts as electrode. In this case, no ring is employed and there is no meniscus effect (Fig. 8).[38] The second procedure uses an aqueous solution of 60% perchloric acid and ethanol (1 : 2) to form a lamella with an Ag ring that acts as a cathode. A silver wire (anode) is then dipped into the lamella and the voltage is applied.[39]

AFM Tips as templates. Another route to prepare metal tips with a very small radius is to employ a sharp AFM tip (diameter under 10 nm) as a template and coat it with the desired metal. Again different methods can be applied.

Probably the easiest method to obtain nanoparticles at the edge of an AFM tip is by evaporation of thin metal films similar to procedures known to provide silver island films.[15]

Another interesting approach is the generation of colloidal nanoparticles at the tip. A suitable example is shown by Wang *et al.*[41] Here, the AFM tip is immersed in a silver colloid solution produced by Tollen's reaction.

It is not only AFM tips that can be used as templates. Also normal optical fibers can be etched similarly to the production of aperture near-field probes to obtain the desired tip shape.[42] Also melt drawing of glass rods provides satisfactory TERS templates.

Post-treatment by focused ion beam (FIB) milling. FIB milling can be used as a post-treatment to shape tips, *e.g.* after electrochemical etching. However, this procedure is currently very expensive. FIB is applied as a technique to produce rational nanostructures required for the specific design of optical nano-antenna. As a sophisticated example, a bow-tie antenna with a nano-gap at the very end of a metal coated AFM tip is shown in Fig. 9.[40] The high precision of FIB allows the control of the length and width of the nanoparticles as antenna structures and in the case of the bow-tie also the gap. By manipulating these parameters, tips for specific excitation wavelengths can be fabricated.

Configurations

One of the main challenges in TERS is the low contrast between the near-field and the far-field signal. As demonstrated by Sun *et al.*[43] for example, the Raman signal coming

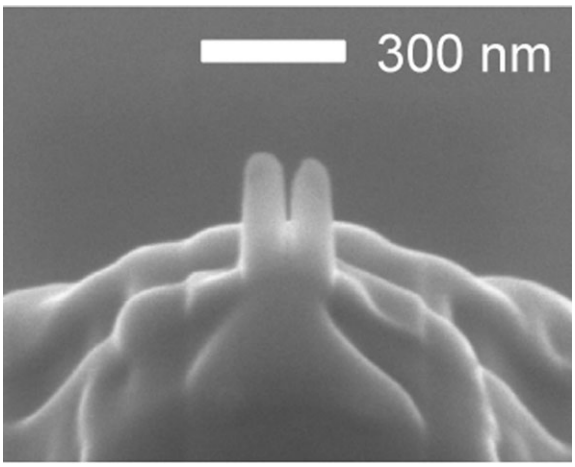

Fig. 9 SEM image of a bow-tie of a metal-coated AFM-tip after FIB milling. Image courtesy of Prof. Dr Hecht, adapted from ref. 40.

from the near-field (enhanced Raman from the tip apex) was estimated to be only 35%, while the rest (65%, unenhanced Raman) was collected from the far-field. This low contrast can be improved by the illumination configuration, which has a major influence on the enhancement properties of the electromagnetic field at the apex of the tip.

Reflection setup. Several modes such as side-illumination and top-illumination could be realized in a reflection setup (see Fig. 10). The major advantage of reflection mode is that the sample can be opaque. A disadvantage is the low contrast between the near-field and far-field signals because of the unfavorable ratio between the illuminated and enhanced areas. This problem can be partly solved by using a suitable polarized configuration.[26,27]

Back-reflection setup. In TERS setups with a back reflection mode, configuration has been discussed already. Here, the tip is illuminated from below using an immersion oil objective with a high numerical aperture. The Raman signal is collected by the same objective. This configuration ensures a high efficiency and avoids a large contribution of unenhanced signal compared to the standard reflection mode. The major shortcoming for this configuration is the restriction to transparent samples.

In conclusion, the choice for the optimal TERS configuration critically depends on the specific requirements of the samples involved. The appropriate illumination mode configuration for a TERS experiment will depend on the transparency of the sample. The choice of the proper tip depends on the spectral absorption characteristics of the sample and therefore which excitation wavelength is desirable. Finally, the feedback system required depends either on the conductivity properties or the thickness of the sample.

Applications

Since the first experimental realization of TERS, several research groups are working in different directions to further improve the technique and also to understand the theoretical background. At the same time TERS is being applied to a multitude of different scientific problems. In the following

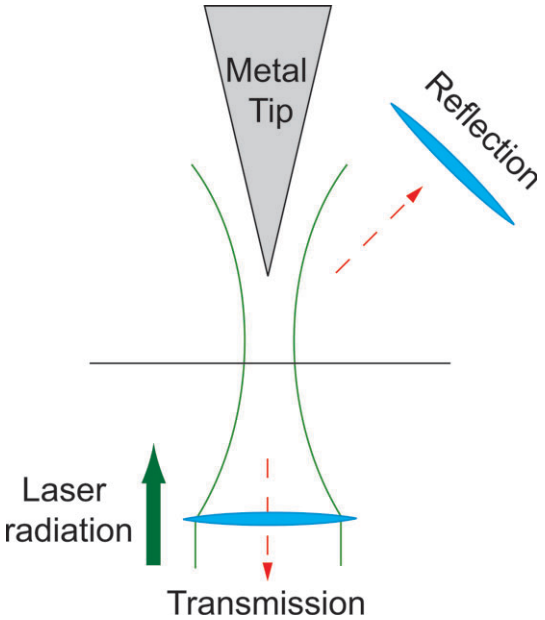

Fig. 10 Schematic diagram of reflection and transmission illumination configuration of TERS experiments.

section, we will present practical examples that cover applications ranging from material analysis to cell biology.

Inorganic materials

Nowadays, the development of integrated circuits (ICs) has been improved by introducing strained silicon inside the channels which induces a faster carrier mobility of the electrons in the transistor channel. Hence, the study of the structure and strain state of the silicon with higher and higher lateral resolution is necessary. Zhu and co-workers[44] demonstrated in a recent report the capacity of TERS to supply structural information at the required spatial resolution. For this purpose a sample composed of strained silicon (sSi) film on a SiO_2 layer above a bulk Si substrate was patterned by FIB milling. Several lines with identical widths and constant depth were milled and were (see Fig. 11) investigated using the TERS technique. In this case, a Cr-coated quartz tip (Nanonics) coated with silver was used in order to avoid background scattering from the tip. The spectra show a double band, at positions around 516 and 520.4 cm^{-1} corresponding to sSi and Si bulk, respectively. Even the 100 nm wide sSi line could be resolved satisfactorily.

This experiment nicely demonstrates the capabilities of TERS in applications related to materials science. Here the samples are most often opaque and only side or top illumination geometries can be used. Nevertheless, the combination of Raman to distinguish specific silicon modifications and near-field optics to provide the necessary lateral resolution allows the identification of features well below the diffraction limit.

Organic compounds

As an example of the investigation of organic materials, TERS experiments of single-walled carbon nanotubes (SWNTs) will be discussed.

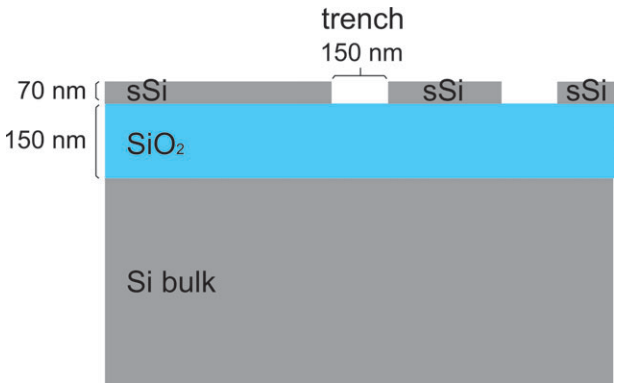

Fig. 11 Schematic diagram of a strained silicon specimen on a silicon target.

Nowadays, single-walled carbon nanotubes (SWNTs) play a significant role in nanotechnology research. They promise a large potential and ample variety for nanotechnological applications. The one-dimensional structure of SWNTs results in characteristic Raman bands: the radial breathing mode (RBM, 100–300 cm^{-1}), the tangential stretching mode (G band, $\sim$1600 cm^{-1}) and the disorder induced mode (D band, $\sim$1300 cm^{-1}).

To demonstrate the high resolution capabilities of the TERS for his particular specimen, we select an example published by Hartschuh.[9] TERS experiments were performed along a single SWCNT, grown by arc discharge using a Ni/Y catalyst, (see Fig. 12) at 4 adjacent positions. At the beginning of the SWCNT, positions 1 and 2, the G band shows a stronger intensity than the G′ band (G/G′ $\approx$ 1.3). By moving the tip

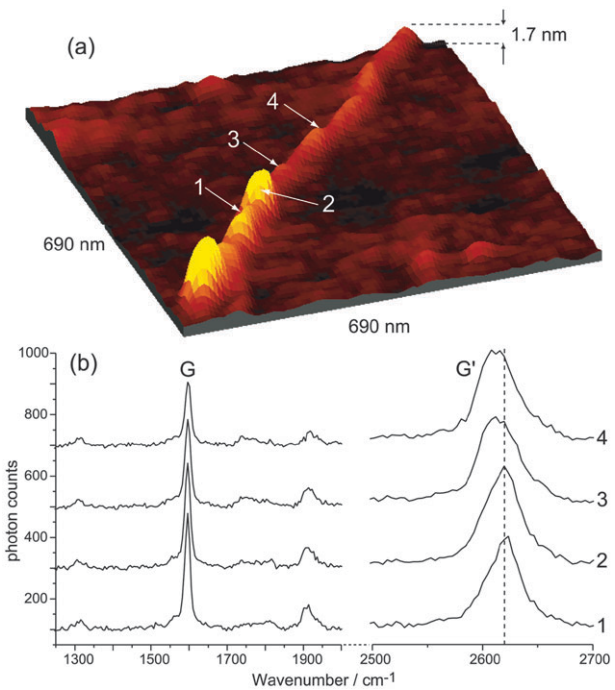

Fig. 12 (a) Three-dimensional topographic image of a single SWNT on glass. (b) Near-field Raman spectra detected at positions 1 to 4 shown in (a). By courtesy of Prof. Dr Achim Hartschuh, adapted from ref. 9.

along the SWCNT (positions 3 and 4), the intensity of the G band decreases with respect to the G′ band (G/G′ ≈ 0.7).

A frequency shift in the band position has not been observed for the G band, but significant strong shifts were detected for the G′ band. The spectral fluctuations represent changes in the SWCNT structure, which can be related to external stress produced by local defects or particles from the catalyst. Such results cannot be provided by any other method and again indicate the potential of the TERS system.[45–47]

Nucleic acid analysis

With respect to applications in the field of bio-organic compounds, it is very tempting to apply the TERS technique, as the amount of sample is usually quite limited and also the precise location of a compound is crucial for a specific biological effect. Here in particular, TERS could be a powerful tool because of its low limits of detection and its high lateral resolution.

A nice example would be the Raman spectroscopic investigation of DNA or RNA. With higher and higher resolution, ultimately a single base sensitivity could be reached. The main challenge for the study of DNA strands by SERS is that the sugar and phosphate groups block the signals of the nucleobases. This is a critical problem for base identification using TERS. To overcome this issue, DNA strands have been labelled with Raman-active dyes and the indirect detection due to hybridisation has been demonstrated by monitoring Raman spectra of the dye-labels.[48,49]

Some TERS studies have already been realized successfully on DNA base nanocrystals.[13,15,50] These studies clearly demonstrate that a distinction between the nucleobases is possible by TERS.

Such experiments can lead to a novel direct sequencing technique. In a recent report, TER spectra along an RNA strand of homopolymer of cytosine have been achieved.[34] This is the first approach towards a direct and label-free Raman sequencing investigation of single-stranded RNA.

RNA strands can be attached on a mica surface *via* phosphate groups, by adding Mg^{2+} cations to the sample. Thus, phosphate groups are bound on the mica surface and the bases become accessible for TERS measurements.[51] The same procedure has been applied to the RNA sample in this particular experiment. Firstly, the sample was scanned with a TERS-tip. The topography image, shown in Fig. 13, obviously corresponds to a single-stranded RNA strand of cytosine.

In the actual TERS experiment, the tip moves to several adjacent positions along the strand. All spectra show the characteristic features of cytosine and are similar, still showing significant fluctuations in band intensities and also slight fluctuations in the band positions (see Fig. 14). The reasons for these features can be explained well by the arguments discussed previously in the theory section.

A closer look at the signal-to-noise ratio of the spectra in comparison with the size of the tip leads to the conclusion that even single-base sensitivity has been achieved, which is one of the prerequisites to perform a direct sequencing using TERS. As the TERS experiments on crystals of the other nucleobases showed specific signals, further experiments with single stranded thymine, adenine, guanine and uracil are expected to complement this experiment.

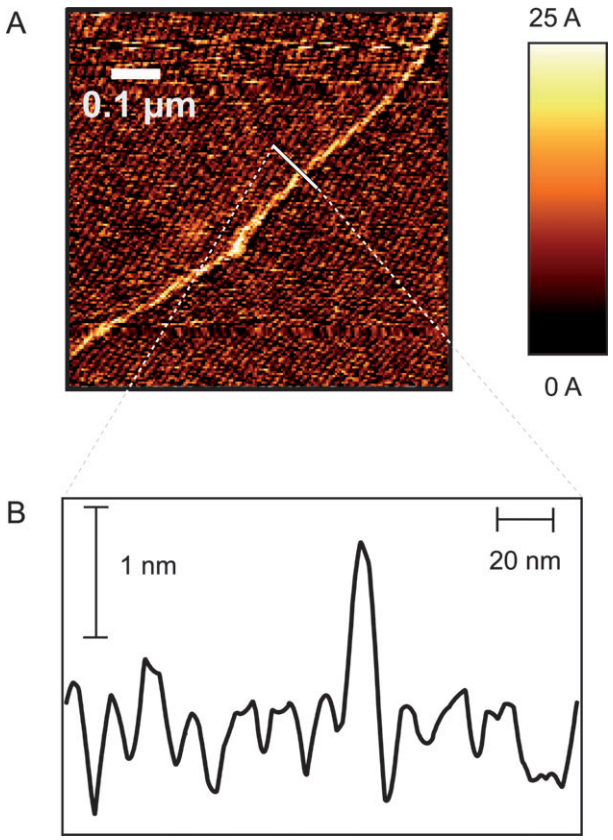

Fig. 13 (A) Topographic image of a cytosine single-stranded RNA homopolymer. (B) Height profile through the RNA at the indicated position. Adapted from ref. 34.

Cells (bacteria)

As an example of even more complex samples, TERS studies on living cells are presented.[52,53] *Staphylococcus epidermidis* is the sample organism used for this TERS experiment. According to the bibliography, the cell surface of *S. epidermidis*, and specifically its cytoplasm membrane, is mainly composed of a peptidoglycan layer, which is pervaded by other polysaccharides and a variety of surface proteins. This is a typical composition of the cytoplasm membrane in all Gram-positive bacteria. It is also likely to find other polysaccharides, *e.g.* teichoic acid or PIA (polysaccharide intercellular adhesion), depending on the growth conditions. Fig. 15 shows the topographic image of *S. epidermidis* cells achieved with an AFM experiment using an ultra sharp silver-coated AFM tip in intermittent mode. The first TER spectra stem from the cell surface—the second spectrum corresponds to a background reference from the glass surface. The enhancement factor was calculated to be around 10^4–10^5. The majority of TERS peaks on the bacteria surface could be tentatively assigned to peptides, lipids and carbohydrates abundant on the cell surface of bacteria.[53] Hence, the TERS experiment provides similar information as previous SERS research on whole cells.[54]

With the ability to perform experiments even on complex organisms, interesting possibilities arise. Applications range

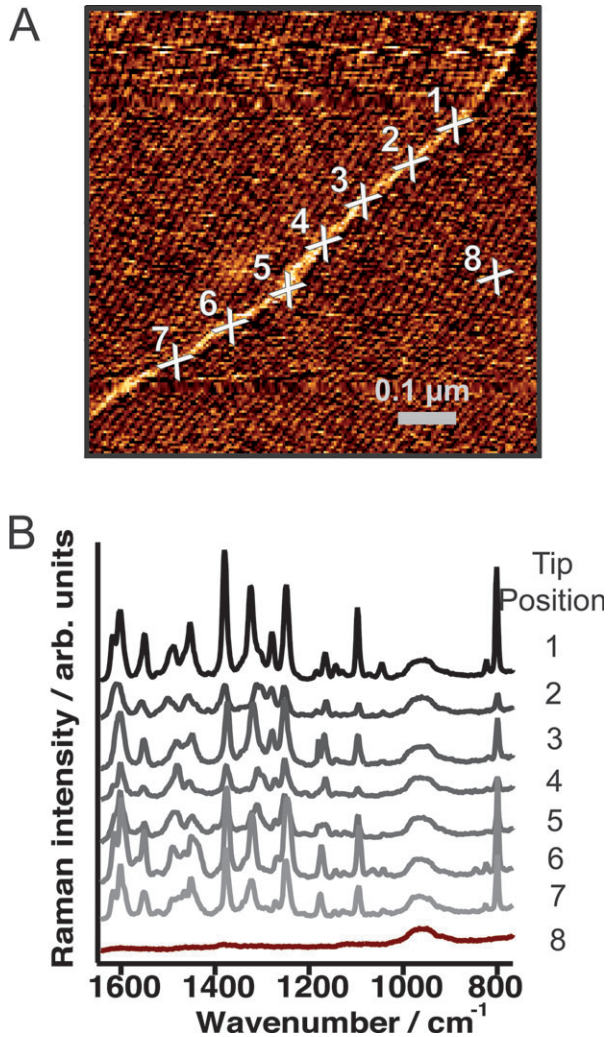

Fig. 14 TERS experiment along a RNA strand. (A) Topographic image (same as Fig. 13A). (B) TERS spectra at the seven adjacent (1–7) spots correspondingly marked in (A), position 8 marks a reference measurement. Adapted from ref. 34.

from a simple reduction in background signals due to the high lateral resolution to the study of diffusion dynamics of single proteins on the cell surface.

Conclusion

Tip-enhanced Raman spectroscopy is a promising tool for the structural investigation of molecules on the nanometre scale. Because the enhancing feature (''the tip'') is always the same during an experiment, quantitative or semi-quantitative experiments are possible with one tip. At present, there is no real alternative when a direct molecular identification is required at the nanometre scale. This is even more the case when comparing TERS with other nanoanalytical tools (SEM, XPS *etc.*). Such techniques often require special environmental conditions. Using Raman and AFM, the two techniques combined for TERS, samples can be investigated over a large range of conditions, as has been demonstrated in the experiment section. Even experiments in liquids (*e.g.* water) are feasible.

Presently the main challenge is a reproducible mass production of the TERS tips. As the tips pick up material during a scan or simply break, this limits the average lifetime to a few days. Hence, TERS tips have to be exchanged more frequently compared to standard AFM probes. Many groups and joint projects are working on the subject of TERS tip production. Ideally, TERS tips would be commercially available like other AFM or SNOM probes.

A very interesting feature is that TERS allows a molecular view on small ensembles of molecules or even single molecules. This would enable a new insight into molecule surface interactions. The ultimate target in terms of applications is the label-free sequencing of biopolymers (DNA, RNA, peptides). The current results are very promising.

Acknowledgements

The authors gratefully acknowledge help on the modelling systems from I. Hellmann, Dresden.

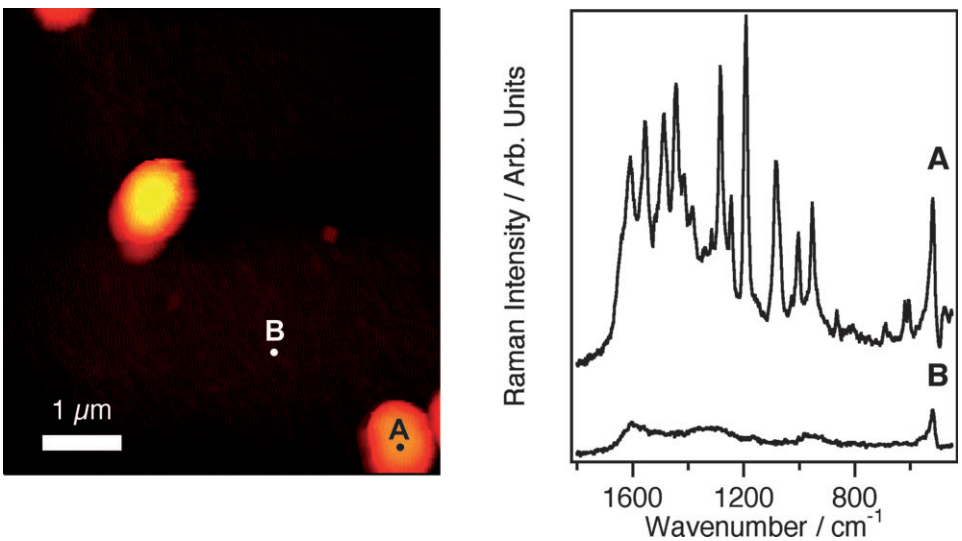

Fig. 15 (a) Topographic image of *S. epidermidis* cells. (b) Tip-enhanced Raman spectra of the marked positions in (a). Position (A) corresponds to a TERS spectrum on the cell surfaces, and position (B) corresponds to a reference TERS experiment on the glass surface. Adapted from ref. 52.

References

1 A. Wokaun, J. P. Gordon and P. F. Liao, *Phys. Rev. Lett.*, 1982, **48**, 957.
2 P. W. Barker, R. K. Chang and H. Massoudi, *Phys. Rev. Lett.*, 1983, **50**, 997.
3 J. E. Wessel, *J. Opt. Soc. Am. B*, 1985, **2**, 1538.
4 S. Nie and S. R. Emory, *Science*, 1997, **275**, 1102.
5 S. R. Emory and S. Nie, *Anal. Chem.*, 1997, **69**, 2631.
6 R. M. Stockle, Y. D. Suh, V. Deckert and R. Zenobi, *Chem. Phys. Lett.*, 2000, **318**, 131.
7 M. S. Anderson, *Appl. Phys. Lett.*, 2000, **76**, 3130.
8 N. Hayazawa, Y. Inouye, Z. Sekkat and S. Kawata, *Opt. Commun.*, 2000, **183**, 333.
9 A. Hartschuh, E. J. Sánchez, X. S. Xie and L. Novotny, *Phys. Rev. Lett.*, 2003, **90**, 095503.
10 B. Pettinger, G. Picardi, R. Schuster and G. Ertl, *Single Mol.*, 2002, **3**, 285.
11 M. Moskovits, *Rev. Mod. Phys.*, 1985, **57**, 783.
12 A. Campion and P. Kambhampati, *Chem. Soc. Rev.*, 1998, **27**, 241.
13 H. Watanabe, Y. Ishida, N. Hayazawa, Y. Inouye and S. Kawata, *Phys. Rev. B: Condens. Matter Mater. Phys.*, 2004, **69**, 155418.
14 P. Verma, K. Yamada, H. Watanabe, Y. Inouye and S. Kawata, *Phys. Rev. B: Condens. Matter Mater. Phys.*, 2006, **73**, 045416.
15 A. Rasmussen and V. Deckert, *J. Raman Spectrosc.*, 2006, **37**, 311.
16 I. Hellmann, *Optische Felverstärkung an metallischen Spitzen*, Technischen Universität Dresden, Dresden, 2003.
17 F. Festy, A. Demming and D. Richards, *Ultramicroscopy*, 2004, **100**, 437.
18 J. T. Krug, E. J. Sanchez and X. S. Xie, *J. Chem. Phys.*, 2002, **116**, 10895.
19 M. Micic, N. Klymyshyn, Y. D. Suh and H. P. Lu, *J. Phys. Chem. B*, 2003, **107**, 1574.
20 Y. C. Martin, H. F. Hamann and H. K. Wickramasinghe, *J. Appl. Phys.*, 2001, **89**, 5774.
21 J. Renger, S. Grafström, L. M. Eng and V. Deckert, *J. Opt. Soc. Am. A*, 2004, **21**, 1362.
22 L. Novotny, R. X. Bian and X. S. Xie, *Phys. Rev. Lett.*, 1997, **79**, 645.
23 B. Hecht, B. Sick, U. P. Wild, V. Deckert, R. Zenobi, O. J. F. Martin and D. W. Pohl, *J. Chem. Phys.*, 2000, **112**, 7761.
24 L. Novotny, M. R. Beversluis, K. S. Youngworth and T. G. Brown, *Phys. Rev. Lett.*, 2001, **86**, 5251.
25 Y. Saito, N. Hayazawa, H. Kataura, T. Murakami, K. Tsukagoshi, Y. Inouye and S. Kawata, *Chem. Phys. Lett.*, 2005, **410**, 136.
26 Q. Nguyen, R. Ossikovski and J. Schreiber, *Opt. Commun.*, 2007, **274**, 231.
27 D. Mehtani, N. Lee, R. D. Hartschuh, A. Kisliuk, M. D. Foster, A. P. Sokolov and J. F. Maguire, *J. Raman Spectrosc.*, 2005, **36**, 1068.
28 A. Bouhelier, M. Beversluis, A. Hartschuh and L. Novotny, *Phys. Rev. Lett.*, 2003, **90**, 013903.
29 A. V. Zayats, T. Kalkbrenner, V. Sandoghdar and J. Mlynek, *Phys. Rev. B: Condens. Matter Mater. Phys.*, 2000, **61**, 4545.
30 S. Kawata and P. Verma, *Chimia*, 2006, **60**, 770.
31 T. Ichimura, N. Hayazawa, M. Hashimoto, Y. Inouye and S. Kawata, *Phys. Rev. Lett.*, 2004, **92**, 220801.
32 K. Ikeda, Y. Saito, N. Hayazawa, S. Kawata and K. Uosaki, *Chem. Phys. Lett.*, 2007, **438**, 109.
33 E. J. Ayars, H. D. Hallen and C. L. Jahncke, *Phys. Rev. Lett.*, 2000, **85**, 4180.
34 E. Bailo and V. Deckert, *Angew. Chem., Int. Ed.*, 2008, **47**, 1658.
35 A. Downes, D. Salter and A. Elfick, *J. Phys. Chem. B*, 2006, **110**, 6692.
36 D. Richards, R. G. Milner, F. Huang and F. Festy, *J. Raman Spectrosc.*, 2003, **34**, 663.
37 B. Ren, G. Picardi and B. Pettinger, *Rev. Sci. Instrum.*, 2004, **75**, 837.
38 K. Dickmann, F. Demming and J. Jersch, *Rev. Sci. Instrum.*, 1996, **67**, 845.
39 L. Zhu, J. Atesang, P. Dudek, M. Hecker, J. Rinderknecht, Y. Ritz, H. Geisler, U. Herr, R. Geer and E. Zschech, *Mater. Sci.-Poland*, 2007, **25**, 19.
40 J. N. Farahani, H.-J. Eisler, D. W. Pohl, M. Pavius, P. Flückiger, P. Gasser and B. Hecht, *Nanotechnology*, 2007, **18**, 125506.
41 J. J. Wang, Y. Saito, D. N. Batchelder, J. Kirkham, C. Robinson and D. A. Smith, *Appl. Phys. Lett.*, 2005, **86**, 263111.
42 R. Stockle, C. Fokas, V. Deckert, R. Zenobi, B. Sick, B. Hecht and U. P. Wild, *Appl. Phys. Lett.*, 1999, **75**, 160.
43 W. X. Sun and Z. X. Shen, *Mater. Phys. Mech.*, 2001, **4**, 17.
44 L. Zhu, C. Georgi, M. Hecker, J. Rinderknecht, A. Mai, Y. Ritz and E. Zschech, *J. Appl. Phys.*, 2007, **101**, 104305.
45 N. Anderson, A. Bouhelier and L. Novotny, *J. Opt. A: Pure Appl. Opt.*, 2006, **8**, S227.
46 A. Hartschuh, H. Qian, A. J. Meixner, N. Anderson and L. Novotny, *J. Lumin.*, 2006, **119–120**, 204.
47 H. Qian, T. Gokus, N. Anderson, L. Novotny, A. J. Meixner and A. Hartschuh, *Phys. Status Solidi B*, 2006, **243**, 3146.
48 K. Faulds, W. E. Smith and D. Graham, *Anal. Chem.*, 2004, **76**, 412.
49 D. Graham, B. J. Mallinder and W. E. Smith, *Biopolymers*, 2000, **57**, 85.
50 K. F. Domke, D. Zhang and B. Pettinger, *J. Am. Chem. Soc.*, 2007, **129**, 6708.
51 H. G. Hansma, I. Revenko, K. Kim and D. E. Laney, *Nucleic Acids Res.*, 1996, **24**, 713.
52 U. Neugebauer, P. Rösch, M. Schmitt, J. Popp, C. Julien, A. Rasmussen, C. Budich and V. Deckert, *ChemPhysChem*, 2006, **7**, 1395.
53 U. Neugebauer, U. Schmid, K. Baumann, W. Ziebuhr, S. Kozitskaya, V. Deckert, M. Schmitt and J. Popp, *ChemPhysChem*, 2007, **8**, 124.
54 R. M. Jarvis, A. Brooker and R. Goodacre, *Anal. Chem.*, 2004, **76**, 5198.